JOURNAL OF BACTERIOLOGY, Dec. 1996, p. 6833–6841 Vol. 178, No. 23
0021-9193/96/$04.00+0

Novel Nuclear Magnetic Resonance Spectroscopy Methods Demonstrate Preferential Carbon Source Utilization by *Acinetobacter calcoaceticus*

GEORGE L. GAINES III,[1]* LUCIAN SMITH,[1] AND ELLEN L. NEIDLE[2]

Isogenetics, Inc., Chicago Technology Park, Chicago, Illinois 60612,[1] and Department of Microbiology, University of Georgia, Athens, Georgia 30602[2]

Received 13 May 1996/Accepted 24 September 1996

Novel nuclear magnetic resonance spectroscopy techniques, designated metabolic observation, were used to study aromatic compound degradation by the soil bacterium *Acinetobacter calcoaceticus*. Bacteria which had been rendered spectroscopically invisible by growth with deuterated (^{2}H) medium were used to inoculate cultures in which natural-abundance ^{1}H hydrogen isotopes were provided solely by aromatic carbon sources in an otherwise ^{2}H medium. Samples taken during the incubation of these cultures were analyzed by proton nuclear magnetic resonance spectroscopy, and proton signals were correlated with the corresponding aromatic compounds or their metabolic descendants. This approach allowed the identification and quantitation of metabolites which accumulated during growth. This in vivo metabolic monitoring facilitated studies of catabolism in the presence of multiple carbon sources, a topic about which relatively little is known. *A. calcoaceticus* initiates aromatic compound dissimilation by forming catechol or protocatechuate from a variety of substrates. Degradation proceeds via the β-ketoadipate pathway, comprising two discrete branches that convert catechol or protocatechuate to tricarboxylic acid cycle intermediates. As shown below, when provided with several carbon sources simultaneously, all degraded via the β-ketoadipate pathway, *A. calcoaceticus* preferentially degraded specific compounds. For example, benzoate, degraded via the catechol branch, was consumed in preference to *p*-hydroxybenzoate, degraded via the protocatechuate branch, when both compounds were present. To determine if this preference were governed by metabolites unique to catechol degradation, pathway mutants were constructed. Studies of these mutants indicated that the product of catechol ring cleavage, *cis*,*cis*-muconate, inhibited the utilization of *p*-hydroxybenzoate in the presence of benzoate. The accumulation of high levels of *cis*,*cis*-muconate also appeared to be toxic to the cells.

Despite extensive research on bacterial hydrocarbon metabolism, little is known about how the presence of multiple carbon sources influences the degradation of an individual compound. In these studies, a new nuclear magnetic resonance (NMR) spectroscopy technique was used to monitor the catabolism of aromatic compound mixtures by the soil bacterium *Acinetobacter calcoaceticus*. This technique, designated metabolic observation NMR (MO-NMR), is based on the principle that NMR spectrometers will not detect deuterated (^{2}H) compounds when tuned to proton (^{1}H) frequencies (11, 14, 20, 32). As described in this report, *A. calcoaceticus* was grown in fully deuterated medium, thereby rendering the bacterial cultures spectroscopically invisible. Mixtures of ^{1}H aromatic compounds were added to the deuterated cultures as sources of carbon and energy, and samples were taken at specific times. NMR spectra of the samples were used to monitor the metabolic fates of the ^{1}H compounds over time; these spectra provided information about the identity and the accumulation of metabolic intermediates derived from the ^{1}H compounds as well as on the kinetics of metabolite flow. Since ^{1}H is the most abundant hydrogen isotope, this method allows metabolic investigation of any compound that contains nonexchangeable hydrogens without requiring specific labeling.

The ^{1}H-carbon sources provided to *A. calcoaceticus* in these studies were each degraded via the β-ketoadipate pathway (Fig. 1) (17, 26). Many compounds are degraded by this route, each converted to either protocatechuate or catechol, both of which serve as the substrates of ring-cleaving dioxygenases. Following ring cleavage, a series of enzymatic reactions generates tricarboxylic acid cycle intermediates. During this process, the metabolite β-ketoadipate enol-lactone is formed from either protocatechuate or catechol (Fig. 1). *A. calcoaceticus* produces two sets of isozymes to metabolize this common intermediate. During growth with compounds that are metabolized to catechol, enzymes encoded by the *catDIJF* genes are induced by *cis*,*cis*-muconate (6, 26). Protocatechuate induces the isofunctional enzymes encoded by the *pcaDIJF* genes needed for the catabolism of compounds converted to protocatechuate (6, 26). In *A. calcoaceticus*, therefore, the pathways for protocatechuate and catechol degradation represent metabolically parallel but distinct branches of the β-ketoadipate pathway.

To date, most studies of the β-ketoadipate pathway have centered on the enzymes, inducers, and transcriptional regulation involved in the degradation of a single carbon source. Such laboratory conditions, however, do not accurately reflect natural bacterial habitats in which numerous carbon sources are present. Recent investigations of *Alcaligenes eutrophus* (1) and *Pseudomonas putida* (23) indicate that in these bacteria benzoate, degraded via the catechol branch of the β-ketoadipate pathway, is degraded in preference to a second carbon source such as acetate or *p*-hydroxybenzoate. The mechanisms governing preferential benzoate consumption, however, have not yet been elucidated.

Understanding catabolic regulation in multinutrient environments requires techniques that can detect the complex array of metabolites produced during the degradation of carbon

* Corresponding author. Phone: (312) 733-5409. Fax: (312) 829-4069. Electronic mail address: glgaines@merle.acns.nwu.edu.

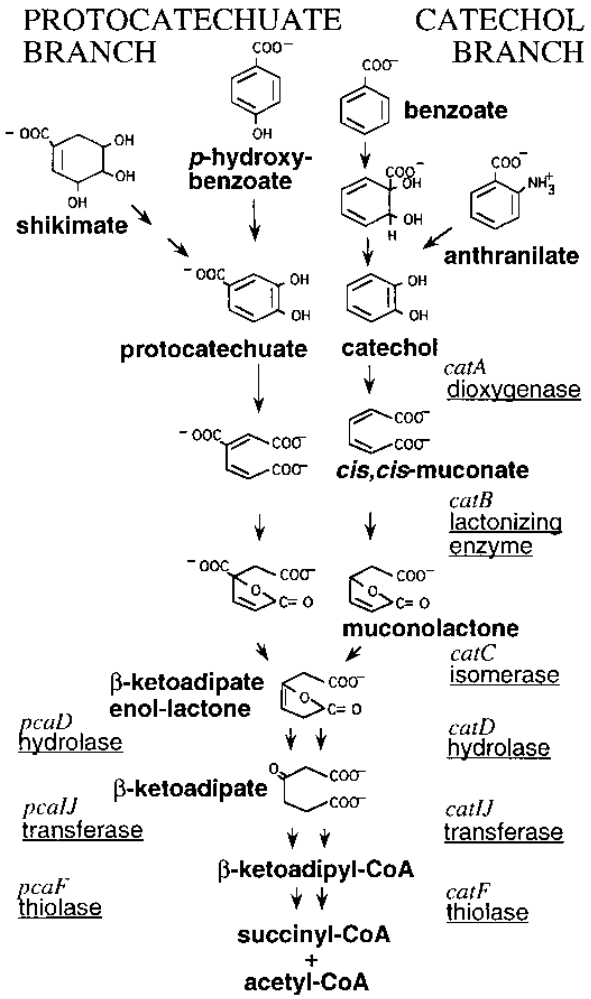

FIG. 1. The protocatechuate and catechol branches of the β-ketoadipate pathway in *A. calcoaceticus*. Compounds, genes, and enzymes are indicated by boldface, italicized, and underlined text, respectively.

source mixtures. The NMR-based techniques described here can provide this information. As shown below, MO-NMR studies of *A. calcoaceticus* demonstrated hierarchical utilization of aromatic carbon sources. Studies of mutant strains identified one metabolite, *cis*,*cis*-muconate, which appears to be involved in regulating preferential benzoate degradation in *A. calcoaceticus.*

MATERIALS AND METHODS

Bacterial strains and plasmids. *A. calcoaceticus* strains and plasmids are shown in Table 1. All *A. calcoaceticus* strains were derived from BD413 (18, 19), here designated ADP1. Two *Escherichia coli* strains, JM101 (36) and DH5α (4), were used as plasmid hosts. Bacteria were cultured at 37°C in ^{1}H medium, either Luria-Bertani broth (31) or minimal medium supplemented with a carbon source as previously described (21, 27).

DNA manipulations and Southern hybridization analyses. Standard methods were used for DNA purifications, subcloning, transformations, and Southern hybridizations (31). Restriction endonucleases and T4 DNA ligase were used as suggested by the supplier, New England Biolabs (Beverly, Mass.). DNA probes for Southern hybridizations were labeled with digoxigenin by random priming, and probes were detected with antidigoxigenin-alkaline phosphatase conjugates and chemiluminescent substrates according to the instructions of the Genius System (Boehringer Mannheim Corp., Indianapolis, Ind.).

Plasmid constructions. Modification of previously isolated plasmids generated pIGG21, pIGG18, and pIGG12 (Table 1). In the following plasmid descriptions, the restriction endonuclease site positions correspond to the 15,923-nucleotide sequence of the *ben-cat* region in GenBank, accession number M76991. *A. calcoaceticus* DNA on plasmid pIB1381 (22) was deleted between the *Sma*I and *Ssp*I sites, positions 4,416 and 5,983, respectively, to generate pIGG21. This deletion eliminated the 5′ end of the *catA* gene and part of an open reading frame upstream of *catA* (25). A deletion, encompassing the *catBCIJFD* genes, between the *Msc*I sites on plasmid pPAN4 (previously designated pAN4) (33), at positions 11,557 and 14,412, generated pIGG18. Plasmid pIGG12 was also derived from pPAN4 (33) by insertion of a DNA fragment from plasmid pHP45 (ΩSp^{r}Sm^r [29]) into the *Sph*I site in *catC*, at position 12,005. The transcriptional and translational stop signals of the ΩSp^{r}Sm^r fragment prevented *catC* expression.

TABLE 1. Bacterial strains and plasmids

Strain or plasmid	Relevant characteristic(s)	Reference(s) or source
A. calcoaceticus strains		
ADP1	Wild type (BD413)	19
ISA13	*catM*::Ω*S4013*	30
ISA16	*catC*::Ω*S4016*	This study
ISA25	Δ*catBCIJF4025*	This study
ISA29	Δ*benE-catA4029*	This study
Plasmids		
pUC19	Ap^r	35, 36
pHP45	Source of Ω*S*	29
pPAN4	Carries *catBCIJFD*	33
pIB1381	Carries *benD-catA*	22
pIGG12	Ω*S* in *catC* of pPAN4	This study
pIGG18	pPAN4 Δ*Msc*I-*Msc*I	This study
pIGG21	pIB1381 Δ*Sma*I-*Ssp*I	This study

Transformation of ADP1 with linear DNA. To the recipient wild-type strain, grown overnight in 5 ml of succinate medium, 10 μl of 1 M succinate was added. After incubation at 37°C for 30 min, 100 μl of the culture and 20 μl of restriction endonuclease-digested plasmid DNA (approximately 0.5 μg) were mixed, and dilutions of the mixture were spread on agar plates. Individual colonies were isolated and screened for the ability to grow with benzoate or *cis*,*cis*-muconate as the sole carbon source. When antibiotics were used to select transformants, the recipient cells and plasmid DNA were diluted with Luria-Bertani broth and allowed to grow for 5 to 12 h prior to being spread on Luria-Bertani agar plates containing antibiotics.

Growth of *A. calcoaceticus* with deuterated media. ^{2}H-IG medium (Isogenetics Inc., Chicago, Ill.) was prepared from algae grown photoautotrophically in deuterated water (>99% ^2H_2O) (11, 32). ^2H_2O was obtained from Ontario Hydro International, Toronto, Canada. With this medium, *A. calcoaceticus* cultures had doubling times of approximately 120 min when grown with aeration at 34°C. A different (defined) deuterated medium, ^{2}H-MM, was prepared by suspending the following ingredients in ^2H_2O: 12.5 mM KH_2PO_4, 12.5 mM Na_2HPO_4, 0.1% $(NH_4)_2SO_4$, and 0.1% concentrated base, pH 6.9. Concentrated base contained 10 g of nitrilotriacetic acid, 30 g of $MgSO_4$, 2.5 g of $CaCl_2$, 9.25 mg of $(NH_4)_6Mo_7O_{24}$, 100 mg of $FeSO_4$, and 50 ml of Hutner's Metals 44 (9) in 500 ml. To support growth, carbon sources were added to ^{2}H-MM, as was a 10% volume of ^{2}H-IG medium to provide additional nutrients apparently required for deuterated growth. As expected, the ^{2}H-IG-supplemented ^{2}H-MM medium was able to support some growth even in the absence of added carbon sources. Under these conditions, wild-type cells reached an approximate density of 10^7 cells per ml, compared with an approximate density of 10^9 cells per ml in the presence of added carbon sources. With aromatic compounds as carbon sources, the doubling times of wild-type cells were approximately 120 min.

Culture conditions for MO-NMR studies. Cultures in ^{2}H-IG medium, inoculated from single colonies on succinate ^{1}H-minimal medium plates, were grown overnight. In the morning, a 100-μl sample of the culture was added to a tube containing 6 ml of ^{2}H-MM and 600 μl of ^{2}H-IG medium. The addition of a carbon source marked the start of an experiment, and 650 μl was taken from the tube and frozen immediately following this addition (zero time point). Carbon sources (^{1}H compounds) were added at the following final concentrations to the deuterated cultures: benzoate and *p*-hydroxybenzoate, 3 mM; anthranilate and shikimate, 1 mM. The cultures were then incubated at 34°C in tubes fixed at an angle of approximately 60° from the horizontal plane of a shaking platform that moved at 300 rpm to provide aeration. Periodically, 650-μl samples were withdrawn and immediately frozen. The samples were kept frozen until NMR analysis. For each mutant, a preliminary test, with time points varying from 4 to 48 h, determined an appropriate window for sampling times. The experiment was then repeated with samples being removed every hour during the determined time window.

MO-NMR spectroscopy. Each sample was thawed to room temperature and immediately transferred to a 5-mm NMR tube with minimal disturbance. Each tube was introduced into a 300-MHz General Electric QE-300 Fourier transform

TABLE 2. NMR spectral signals

Compound	Type of signal	Location(s) of signal (ppm)
Starting compounds		
Benzoate	Doublet	7.9
	Multiplet	7.5–7.6
p-Hydroxybenzoate	Doublet	7.8
	Doublet	6.9
Shikimate	Broad singlet	6.45
	Broad singlet	4.40
	Doublet of doublets	3.9–4.05
	Doublet of doublets	3.65–3.8
	Doublet of doublets	2.65–2.85
	Doublet of doublets	2.1–2.3
Anthranilate	Multiplet	7.2–7.35
	Doublet	7.68
	Multiplet	6.8–7.0
Metabolites		
cis,*cis*-Muconate	Doublet	5.95
	Doublet	6.9
Protocatechuate	Multiplet	7.33–7.45
	Doublet	6.86–6.96
β-Ketoadipate	Two peaks	2.35–2.44
	Broad multiplet	2.75–2.9
Muconolactone	Doublet	7.8
	Doublet	6.2
	Doublet	5.6
	Doublet	2.5

(FT) spectrometer, spun at approximately 20 Hz, and manually shimmed. A presaturation pulse sequence was used, and the decoupling pulse was centered at the residual ^{1}H water peak (4.80 ppm). Approximately 2 min elapsed between the transfer of the sample to the NMR tube and the start of data acquisition. A 4-min acquisition time consisting of 80 pulses incorporating a pulse angle of 45° to ensure full relaxation of the metabolites was used. After transfer of the free induction decays to a Quadra 630 or IIci Macintosh computer (Apple Computer, Inc., Cupertino, Calif.), MacFID software (Tecmag, Inc., Houston, Tex.) was used for spectral analyses. Line broadening of 1.5 Hz was applied during an exponential multiplication of the free induction decays prior to Fourier transformations. Spectral interpretation was based on comparisons with the spectra of known compounds and on predictions assuming deuteration at specific sites. The positions of signals in NMR spectra which correspond to compounds involved in these studies are provided in Table 2.

Concentrations of specific compounds were determined by integrating selected peaks or sets of peaks that were well separated from other peaks. The integrations were carried out with MacFID software, and the resulting peak areas were normalized with respect to the number of protons. The areas were then compared with the areas corresponding to known concentrations of compounds. Comparisons of multiple samples containing the same concentrations of compounds at time zero indicated only minor variations in peak areas.

Chemicals. *cis*,*cis*-Muconate was a gift from Celgene Corp., Warren, N.J. All other chemicals were purchased from the Aldrich Chemical Co. Inc., Milwaukee, Wis.

RESULTS

Preferential utilization of benzoate when provided with *p*-hydroxybenzoate. Benzoate and *p*-hydroxybenzoate are degraded via the catechol and protocatechuate branches of the β-ketoadipate pathway, respectively (Fig. 1) (17). The MO-NMR techniques described above were used to monitor fully deuterated wild-type *A. calcoaceticus* cultures provided with benzoate, *p*-hydroxybenzoate, or a mixture of the two compounds as carbon sources. Samples were taken at specified times following the addition of the ^{1}H-carbon sources, and the NMR spectra of these samples are shown in Fig. 2. The positions of NMR signals characteristic of benzoate and *p*-hydroxybenzoate are listed in Table 2.

Approximately 30% of the benzoate was consumed within the 5-h period following its addition to the culture (Fig. 2a and d). After this time, the remaining benzoate was rapidly consumed until no benzoate could be detected at all in the sample taken at 8 h. The limit of detection for an individual metabolite under these conditions was estimated to be 50 μM. Small signals corresponding to those of *cis*,*cis*-muconate and β-ketoadipate (Table 2) were observed. Variable amounts of these compounds, from 0 to 0.2 mM, were detected in repetitions of this experiment in samples taken 5 to 10 h after the addition of benzoate to the culture. Signals from other intermediates were not observed.

When 3 mM *p*-hydroxybenzoate alone was provided to the culture (Fig. 2b and d), it was completely consumed within 7 h. No metabolic intermediates were detected during this process. The time needed for the complete degradation of *p*-hydroxybenzoate was similar to that for benzoate degradation, approximately 7 to 8 h. When a mixture of both compounds was provided, however, benzoate was preferentially degraded. Benzoate was consumed within 8 h, as it was when provided alone, whereas *p*-hydroxybenzoate catabolism was delayed (Fig. 2c and d). The amount of *p*-hydroxybenzoate in the 8-h sample following addition of both carbon sources was approximately 75% of its initial level, indicating that the majority of the *p*-hydroxybenzoate was not degraded until benzoate had been completely consumed. The remaining *p*-hydroxybenzoate was rapidly consumed within 2 h following the completion of benzoate degradation. These results suggested that either benzoate or its metabolic descendants were involved in inhibiting *p*-hydroxybenzoate utilization.

Four carbon sources provided. Although benzoate was the preferred carbon source in the two-compound mixture, its consumption was delayed by the additional presence of anthranilate and shikimate, degraded via the catechol and protocatechuate branches of the β-ketoadipate pathway, respectively (Fig. 1) (17). The spectra of samples from a deuterated wild-type ADP1 culture provided with (^{1}H) benzoate, *p*-hydroxybenzoate, anthranilate, and shikimate are shown in Fig. 3. Whereas benzoate provided alone or with *p*-hydroxybenzoate was completely consumed within 8 h (Fig. 2), approximately 90% of the benzoate provided as part of the four-compound mixture remained undegraded in the culture at 8 h. After this time, however, benzoate was rapidly consumed, and by 10.5 h, no benzoate was detected.

In this experiment, the first NMR signals to decrease in intensity over time corresponded to those of shikimate, followed closely by anthranilate (Fig. 3; Table 2). Nevertheless, during the first 7 to 8 h the rates of shikimate and anthranilate utilization were relatively low compared with the rapid rate of benzoate consumption once utilization commenced. It was difficult to assess whether shikimate, anthranilate, or both were initially being used as sources of carbon and energy, because metabolites derived from both shikimate and anthranilate accumulated in the culture. Since all spectral signals stem from the only protons provided, the four added carbon sources, the protocatechuate, *cis*,*cis*-muconate, and β-ketoadipate which accumulated during the first 7 h should have resulted from shikimate and anthranilate metabolism. During this time, the benzoate and *p*-hydroxybenzoate levels did not change significantly. Shikimate and anthranilate were the likely sources of protocatechuate and *cis*,*cis*-muconate, respectively. The specific source(s) of the β-ketoadipate, an intermediate in the degradation of all four carbon sources, however, could not be determined.

The *p*-hydroxybenzoate was not consumed during the 10.5 h following its addition to the culture. The *p*-hydroxybenzoate and all of the intermediary metabolites compounds were, however, ultimately degraded, as indicated by analysis of a sample

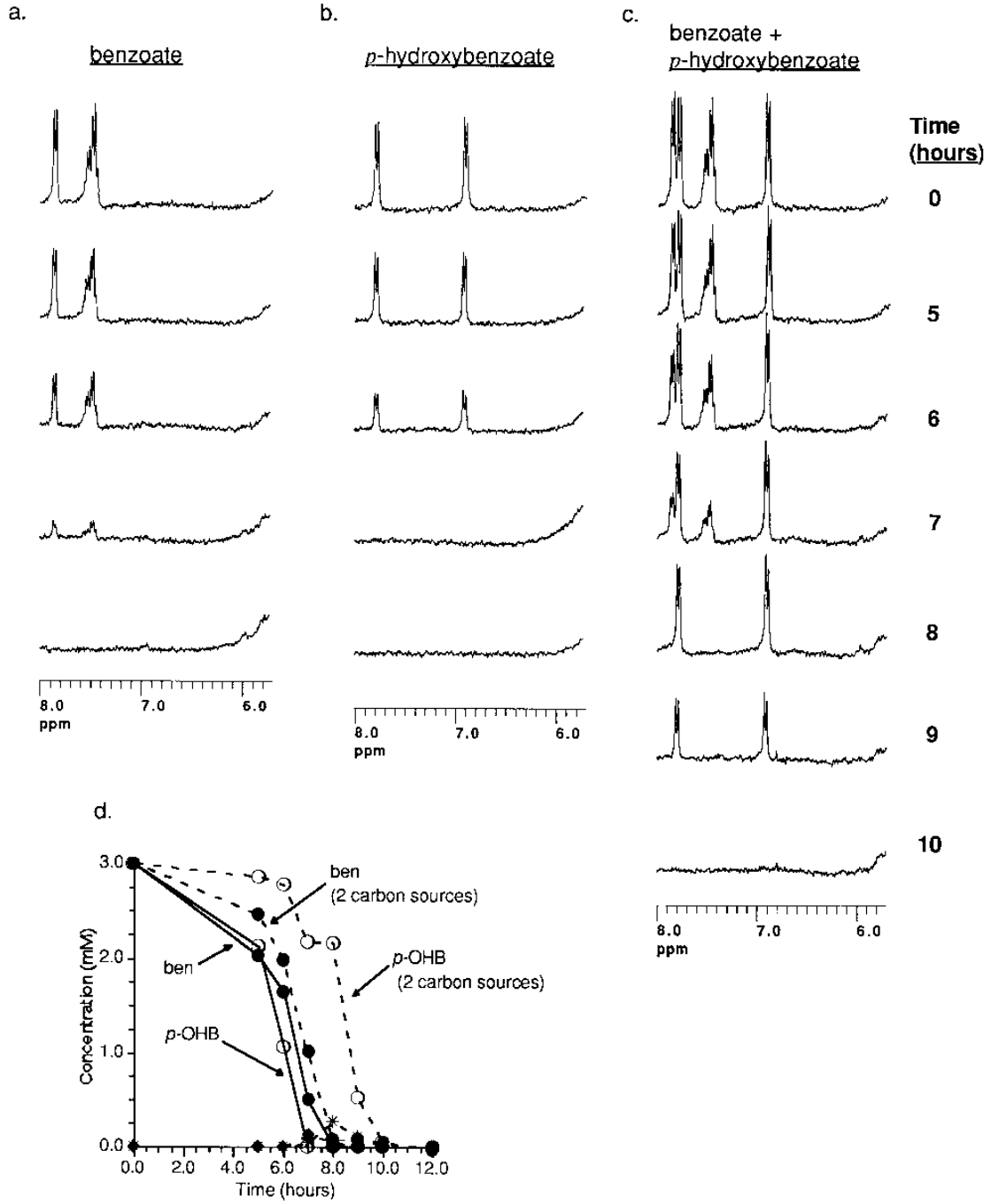

FIG. 2. Individual NMR spectra (aromatic region) of aliquots taken, at indicated times, from fully deuterated cultures of ADP1 which were provided at hour 0 with ^{1}H-carbon sources: 3 mM benzoate (a), 3 mM *p*-hydroxybenzoate (b), or 3 mM benzoate and 3 mM *p*-hydroxybenzoate (c). (d) Concentrations of benzoate (ben), *p*-hydroxybenzoate (*p*-OHB), *cis*,*cis*-muconate (diamonds), and β-ketoadipate (stars) were calculated by integration of NMR spectral peaks. Samples were provided with a single carbon source (panels a and b and solid lines in panel d) or with two carbon sources (panel c and dashed lines in panel d).

taken at 24 h (Fig. 3). The utilization of *p*-hydroxybenzoate may have been inhibited by metabolites generated during the degradation of benzoate or anthranilate via the catechol branch of the β-ketoadipate pathway. There are three compounds specific to the catechol branch of the pathway: catechol, *cis*,*cis*-muconate, and muconolactone (Fig. 1). In order to determine if any of these compounds inhibited *p*-hydroxybenzoate utilization, mutants that were blocked in the metabolism of each of these three compounds were constructed.

Construction of mutants unable to degrade catechol. Mutations were constructed in the *catA*, *catB*, and *catC* loci such that benzoate catabolism would be blocked following the formation of catechol, *cis*,*cis*-muconate, and muconolactone, respectively (Fig. 1). With these mutants, it could be determined whether the accumulation of, or the inability to form, any of the catechol branch metabolites affected the utilization of *p*-hydroxybenzoate. The first step in making the chromosomal mutations was the construction of plasmids carrying specifically altered

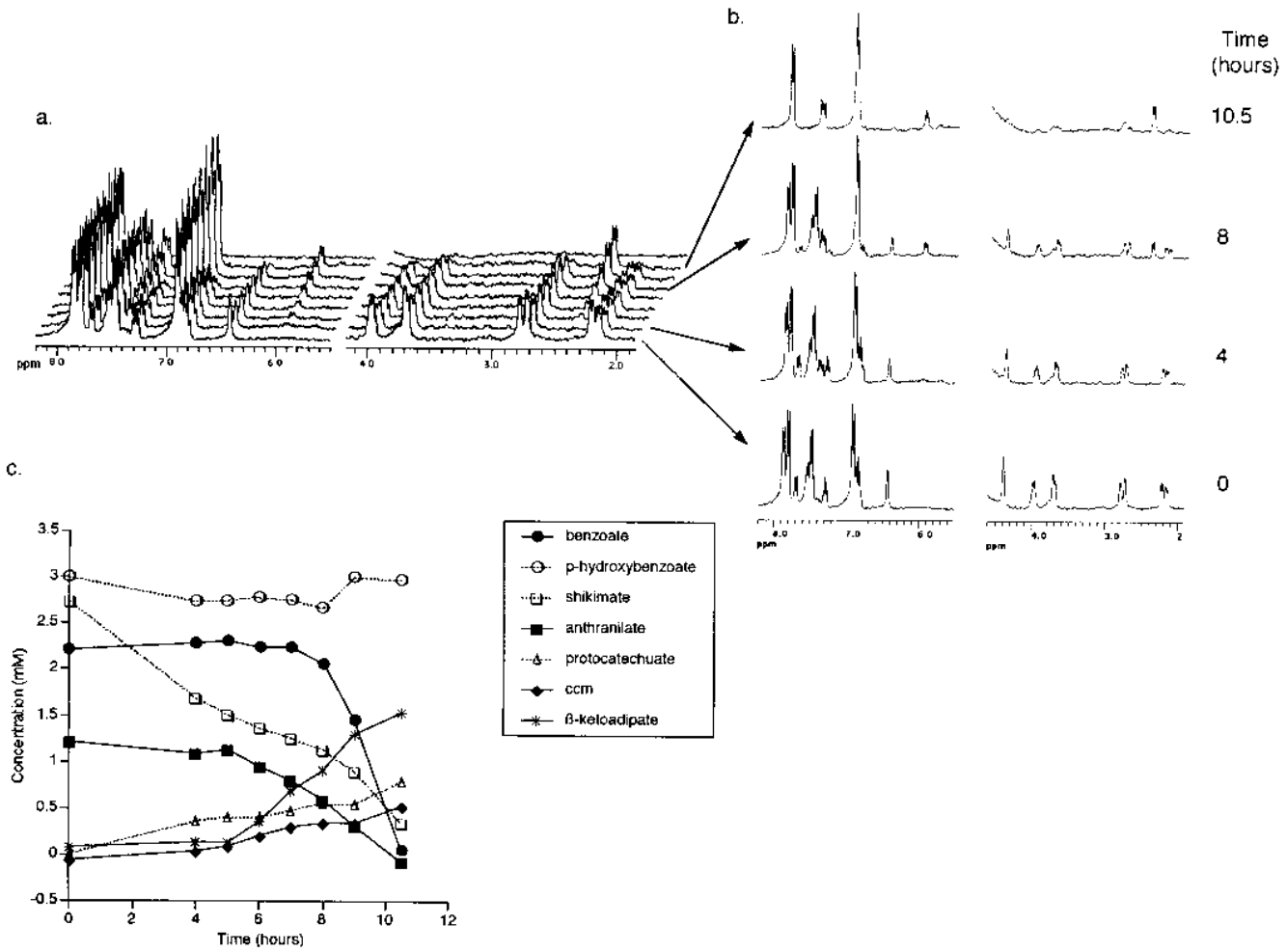

FIG. 3. NMR spectra of samples taken at 0, 4, 5, 6, 7, 8, 9, 10.5, and 24 h after the addition of four ^{1}H compounds, benzoate, *p*-hydroxybenzoate, shikimate, and anthranilate, to a deuterated ADP1 culture. Spectra are shown in chronological order from 0 h (front) to 24 h (back) in panel a, with selected spectra shown in panel b. The region of the spectra around the residual water peak was removed for simplification. For peak identification, see Table 2. The concentrations of the added carbon sources and of metabolites derived from them in the 0- to 10.5-h samples were calculated by integration of the NMR peaks and are shown in panel c as indicated in the box (ccm, *cis*,*cis*-muconate).

cat genes, as described in Materials and Methods. Linearized plasmid DNA was used to transform the naturally competent *A. calcoaceticus* strain ADP1, and transformants in which the mutated genes replaced the wild-type chromosomal alleles were isolated. The construction of the three mutant strains is described below.

Plasmid pIGG21, carrying a deletion of the *catA* gene, was digested with restriction endonuclease *Kpn*I and used to transform ADP1. A resultant transformant, strain ISA29, was isolated and determined to have lost the ability to grow with benzoate or anthranilate as the sole carbon source. In a separate experiment, plasmid pIGG18, with a deletion encompassing the *catBCIJF* genes, was digested with restriction endonuclease *Eco*RI and used to transform ADP1. A transformant designated ISA25 had lost the ability to grow with either benzoate, anthranilate, or *cis*,*cis*-muconate as the sole carbon source. A third mutant was generated by insertional inactivation of *catC*. Plasmid pIGG12, with an ΩSp^rSm^r fragment disrupting *catC*, was digested with endonuclease *Eco*RI and used to transform ADP1. Strain ISA16 was selected as an Sp^rSm^r transformant. Southern hybridization methods confirmed that ISA29, ISA25, and ISA16 had the expected chromosomal mutations in the *catA*, *catB*, and *catC* regions, respectively.

Accumulation of metabolic intermediates and inhibition of *p*-hydroxybenzoate utilization in *catB* and *catC* mutants. In strain ISA16, the *catC* disruption (Fig. 1) did not affect the utilization of *p*-hydroxybenzoate provided alone, as determined by MO-NMR experiments in which the wild-type and ISA16 strains were indistinguishable (data not shown). In MO-NMR experiments in which both benzoate and *p*-hydroxybenzoate were provided, however, ISA16 carried out the conversion of benzoate to muconolactone prior to degrading *p*-hydroxybenzoate, despite the inability to derive energy from benzoate metabolism (Fig. 4a; Table 2). The *p*-hydroxybenzoate was rapidly degraded after most of the benzoate had been converted to muconolactone. In ISA16, as in the wild-type strain, the presence of benzoate or the metabolite(s) derived from it appeared to inhibit *p*-hydroxybenzoate utilization. High sustained levels of muconolactone did not prevent *p*-hydroxybenzoate from ultimately being consumed.

In similar MO-NMR experiments with strain ISA25, which cannot degrade *cis*,*cis*-muconate, it was shown that the chromosomal deletion had no effect on the utilization of *p*-hydroxy-

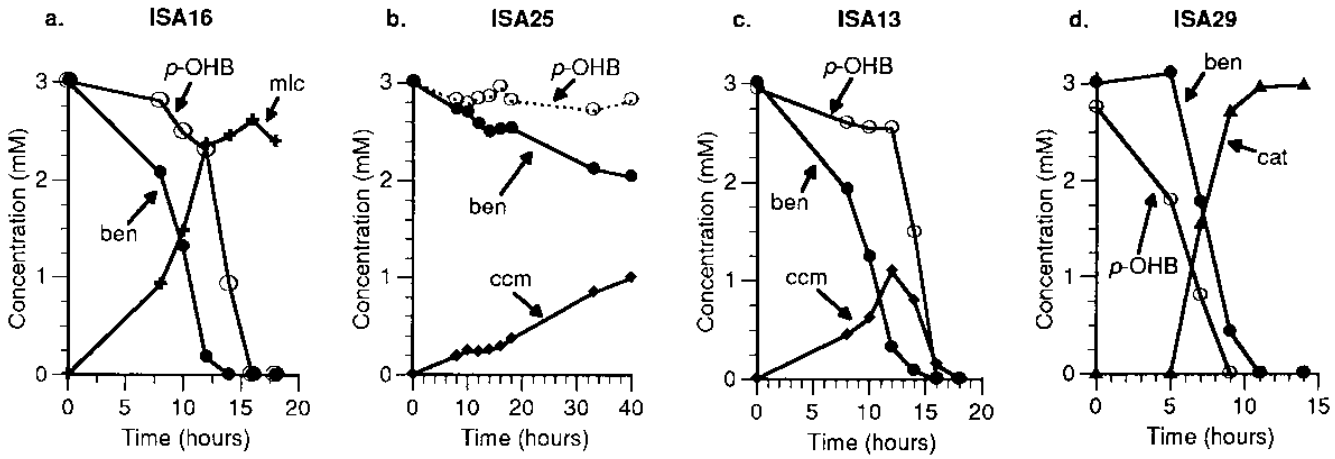

FIG. 4. Addition of 3 mM ^{1}H benzoate and 3 mM ^{1}H *p*-hydroxybenzoate at 0 h to deuterated cultures of mutant strains ISA16 (a), ISA25 (b), ISA13 (c), and ISA29 (d). Concentrations of benzoate (ben), *p*-hydroxybenzoate (*p*-OHB), muconolactone (mlc), *cis*,*cis*-muconate (ccm), and catechol (cat) were calculated by integration of NMR spectral peaks.

benzoate when provided alone (data not shown). When provided with benzoate, however, *p*-hydroxybenzoate was not consumed at all by ISA25 (Fig. 4b). In addition, no growth of the culture was observed. Some benzoate was converted to *cis*,*cis*-muconate, but even after 40 h following the addition of the ^{1}H compounds, approximately 70% of the benzoate remained undegraded in the culture. ISA25 was unable to use *p*-hydroxybenzoate as the source of carbon and energy in the presence of benzoate. In addition, the presence of benzoate prevented ISA25 from using other growth substrates. ISA25 did not grow with ^{1}H minimal medium supplemented with succinate or glucose if benzoate was present.

These results suggested a role for *cis*,*cis*-muconate in inhibiting *p*-hydroxybenzoate degradation and/or that the accumulation of *cis*,*cis*-muconate from benzoate was toxic. To further characterize the role of *cis*,*cis*-muconate in *p*-hydroxybenzoate consumption, we studied a regulatory mutant, ISA13, in which, as shown below, *cis*,*cis*-muconate accumulated to high, but nonlethal, levels. Strain ISA13 carries an insertion in the *catM* regulatory gene which results in decreased expression of the *catB-F* genes needed for *cis*,*cis*-muconate degradation (30). Strain ISA13 can utilize benzoate as the sole source of carbon, but it grows slowly compared with the wild type (30). MO-NMR experiments demonstrated that, unlike the wild type, ISA13 accumulated *cis*,*cis*-muconate to high levels during growth with benzoate (Fig. 5). This *cis*,*cis*-muconate was ultimately completely degraded by ISA13 even though the time required for the complete mineralization of benzoate was much longer than that for the wild type (Fig. 2 and 5).

The results of MO-NMR experiments in which ISA13 was provided with both benzoate and *p*-hydroxybenzoate are shown in Fig. 4c. Despite the long time needed for benzoate degradation, the *p*-hydroxybenzoate was not utilized until most of the benzoate had been consumed and until the accumulated *cis*,*cis*-muconate levels started to decline. After *p*-hydroxybenzoate degradation commenced, it proceeded rapidly to completion. In contrast, the conversion of approximately 1 mM benzoate to 1 mM *cis*,*cis*-muconate by strain ISA25, which cannot further degrade this intermediate, appeared to prevent the consumption of *p*-hydroxybenzoate (Fig. 4b). Although ISA13 also accumulated *cis*,*cis*-muconate to levels as high as 1 mM, *p*-hydroxybenzoate consumption was delayed but not prevented. ISA13 was able to remove all of the accumulated *cis*,*cis*-muconate from the culture within approximately 18 h (Fig. 4c). As discussed below, these results are consistent with *cis*,*cis*-muconate playing a role in inhibiting *p*-hydroxybenzoate degradation.

Conversion of benzoate to catechol by a *catA* mutant with no inhibition of *p*-hydroxybenzoate utilization. In contrast to the behavior of ADP1, ISA16, ISA25, and ISA13, a strain carrying a *catA* deletion, ISA29, exhibited no delay in *p*-hydroxybenzoate utilization in the presence of benzoate. Moreover, MO-NMR experiments indicated that in this strain the initial removal of *p*-hydroxybenzoate from the culture commenced prior to that of benzoate (Fig. 4d). The consumption of *p*-hydroxybenzoate was not inhibited by the presence of benzoate in the ISA29 culture, and *p*-hydroxybenzoate was consumed as rapidly as when provided alone. Benzoate was quantitatively converted to catechol (Fig. 4d). As discussed below, these results suggested that the *catA* mutation blocked formation of a compound(s) involved in inhibiting *p*-hydroxybenzoate catabolism.

DISCUSSION

Individual compounds in a mixture are consumed according to a preferred hierarchy. *A. calcoaceticus* ADP1 consistently

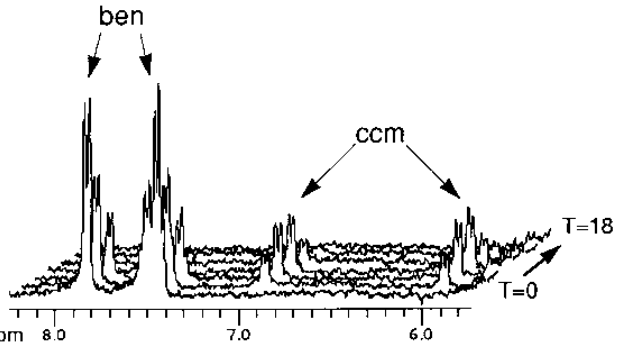

FIG. 5. NMR spectra (aromatic region) of samples taken at 0, 8, 10, 12, 14, 16, and 18 h after the sole addition of ^{1}H benzoate to a deuterated culture of *catM* strain ISA13. Spectra are shown in chronological order from front (0 h) to back (18 h). Peaks corresponding to benzoate (ben) and *cis*,*cis*-muconate (ccm) are indicated.

consumed benzoate prior to *p*-hydroxybenzoate in the presence of both carbon sources. Benzoate, or metabolites derived from it, appeared to delay the start of *p*-hydroxybenzoate degradation by inhibiting its first step, which is catalyzed by an inducible hydroxylase encoded by the *pobA* gene. In studies of *pobA* expression, DiMarco et al. showed that benzoate could slightly reduce the ability of *p*-hydroxybenzoate to induce *pobA* expression (13). The low level of reduction (<10%), however, suggests that transcriptional regulation alone is not responsible for preferential benzoate consumption and/or that benzoate itself is not the principal regulatory metabolite. Moreover, temporal regulatory factors need to be considered, since the extent of benzoate catabolism, the relative concentrations of both carbon sources, and the timing of carbon source addition may control the extent of the inhibition of *pobA* expression.

Nichols and Harwood compared cultures of *P. putida* grown with either benzoate and *p*-hydroxybenzoate or *p*-hydroxybenzoate alone (23). The presence of benzoate resulted in lower activity levels of both *p*-hydroxybenzoate hydroxylase (PobA), which forms protocatechuate, and the subsequent enzyme which cleaves protocatechuate, protocatechuate 3,4-dioxygenase (23). In *A. calcoaceticus*, the activities of these two enzymes may similarly regulate the metabolic flow of multiple carbon sources. In the presence of the four carbon sources studied here, the accumulation of protocatechuate from shikimate was observed (Fig. 3). After 10.5 h, approximately 25% of the shikimate initially present had been converted to protocatechuate but was not yet further catabolized, suggesting that protocatechuate cleavage was rate limiting. The total amount of shikimate which had not yet been utilized as a source of carbon and energy may have been even higher, since some of the accumulating β-ketoadipate may have derived from shikimate. The carbon sources studied here were utilized in a hierarchical fashion with the same consumption order consistently repeated (Fig. 3). In all cases, the inhibition of *p*-hydroxybenzoate utilization in the presence of compounds degraded via the catechol branch of the pathway was striking.

Identification of *cis*,*cis*-muconate as a regulatory metabolite. Studies of *cat* mutants indicated that *cis*,*cis*-muconate is involved in inhibiting *p*-hydroxybenzoate degradation. Benzoate catabolism commenced prior to *p*-hydroxybenzoate catabolism in all strains examined except the *catA*-deleted ISA29 (Fig. 4d), in which the conversion of benzoate to an inhibitory metabolite(s) appeared to be prevented. Such a metabolite would likely be *cis*,*cis*-muconate or muconolactone, since any intermediates beyond muconolactone would be common to *p*-hydroxybenzoate degradation (Fig. 1). In the *catC* mutant ISA16, benzoate was converted to muconolactone prior to *p*-hydroxybenzoate degradation, even though energy could not be derived from this process. ISA16 forms both *cis*,*cis*-muconate and muconolactone. Either or both of these compounds could have inhibited *p*-hydroxybenzoate degradation, although the high sustained level of muconolactone did not prevent *p*-hydroxybenzoate from ultimately being completely degraded. Only a small amount of *cis*,*cis*-muconate, not more than 50 μM, was detected in this experiment, but a transient localized accumulation may have blocked *p*-hydroxybenzoate utilization until *cis*,*cis*-muconate was converted to muconolactone. This possibility is consistent with the complete prevention of *p*-hydroxybenzoate utilization in ISA25 by the conversion of benzoate to *cis*,*cis*-muconate, a metabolite that in this mutant does not get removed by further catabolism.

The inability of ISA25 to degrade *p*-hydroxybenzoate might be caused by *cis*,*cis*-muconate toxicity rather than specific regulation of the β-ketoadipate pathway. Such toxicity could account for benzoate preventing ISA25 from growing with carbon sources such as succinate and glucose. Nevertheless, accumulations of *cis*,*cis*-muconate being harmful and playing regulatory roles are not mutually exclusive possibilities. The high levels of *cis*,*cis*-muconate which accumulated in strain ISA13 were not lethal but appeared to inhibit *p*-hydroxybenzoate consumption. The long delay in *p*-hydroxybenzoate degradation by this mutant corresponded to the delayed catabolism of *cis*,*cis*-muconate. The detected levels of *cis*,*cis*-muconate, however, did not always correspond directly to regulatory effects. For example, the preferential utilization of benzoate or *p*-hydroxybenzoate was determined within the first few hours after carbon source addition (Fig. 2 and 4), during a time when *cis*,*cis*-muconate was not always identified by MO-NMR techniques. As described below, regulation may be governed by localized metabolite concentrations which would not have been detected in these experiments.

Location of compounds detected by MO-NMR. The compounds detected in these MO-NMR experiments were most likely in the medium rather than within the cells even though the entire culture was examined spectroscopically. Consistent with this prediction, analysis of the medium again after the bacterial cells were removed from several samples did not result in significant diminution of the NMR signals (data not shown). Mechanisms of transport for compounds of the β-ketoadipate pathway and the relationships between internal and external metabolite concentrations are not yet known. MO-NMR can be used to detect the internal metabolite concentrations of cells which have been separated from the culture medium, provided that sufficient cellular material is available for NMR analysis.

Utilization of *cis*,*cis*-muconate as a carbon source. *cis*,*cis*-Muconate provided exogenously to ADP1 as a carbon source did not inhibit the degradation of *p*-hydroxybenzoate (data not shown). In this case, *cis*,*cis*-muconate may be taken into the cell concomitant with its degradation such that high internal levels of this compound do not accumulate. In contrast, benzoate degradation may lead to internal accumulations of *cis*,*cis*-muconate that can repress *p*-hydroxybenzoate catabolism. It is also possible that the inhibitory role of *cis*,*cis*-muconate requires other metabolites, such as benzoate, benzoate diol, and/or catechol, such that the presence of *cis*,*cis*-muconate is necessary but not sufficient for inhibition. Two transcriptional activators, BenM (10) and CatM (30), regulate benzoate degradation in response to *cis*,*cis*-muconate. This compound induces all of the enzymes needed for catechol degradation in *A. calcoaceticus*, and it also regulates the conversion of benzoate to catechol (10). CatM was not needed for the inhibition of *p*-hydroxybenzoate utilization in the presence of benzoate, since this still occurred in the *catM* mutant ISA13. Whether BenM is needed for this inhibition remains to be determined.

Metabolite channeling: efficient utilization of carbon sources. The inability to detect most metabolites of the wild-type strain during catabolism may reflect efficient channeling of metabolites through the β-ketoadipate pathway. The genes needed for the catabolism of aromatic compounds are arranged in two distinct chromosomal clusters (16), and the organization within these regions may contribute to tight transcriptional control of adjacent genes or operons. In addition, this genetic arrangement may facilitate the proximal association of proteins with related functions, contributing to the efficient funneling of metabolites through each branch of the pathway. In mutants ISA16 and ISA29, benzoate was quantitatively converted to muconolactone and catechol, respectively. Neither muconolactone nor catechol, therefore, appears to be a feedback inhibitor of benzoate degradation. In strain ISA25, however, only approximately 30% of the benzoate was

converted to *cis*,*cis*-muconate. This might result from specific feedback inhibition mediated by *cis*,*cis*-muconate, the inability to generate energy from *p*-hydroxybenzoate degradation, the toxicity of *cis*,*cis*-muconate, or some combination of these factors.

MO-NMR analysis of metabolism. In this paper, we describe MO-NMR spectroscopy, a new technique in which the full deuteration of microbial cultures renders them invisible to proton NMR spectroscopy. After the addition of unlabeled natural-abundance ^{1}H compounds to the deuterated culture, metabolism can be monitored spectroscopically. Detectable proton signals originate only from the added compounds, any metabolites derived from them, or the residual water peak. High deuteration levels (>95%) are needed to significantly reduce the ^{1}H signals present in the cell material and medium. The full deuteration of organisms, which can be readily accomplished with many strains of bacteria, algae, and yeast (15), requires specialized growth medium. There may be physiological consequences of deuteration, and some microorganisms grow poorly with deuterated medium (15), perhaps because enzymatic reactions involving ^{2}H rather than ^{1}H compounds are adversely affected. *A. calcoaceticus* grew at a reduced rate in deuterated medium, with a doubling time of approximately 120 min, compared with wild-type doubling times in ^{1}H media of approximately 30 to 90 min. Despite the physiological effects of deuteration, these MO-NMR methods permit in vivo metabolite monitoring not possible with other techniques. In variations of the methods described here, the cells and the surrounding culture medium can be analyzed independently, cultures may be incubated directly in the spectrometer with continuous data acquisition, or, alternatively, the activities of cell extracts made from deuterated cultures can be determined. Compared to chromatographic techniques, NMR sampling times of several minutes are relatively short, and analyses of the NMR spectra allow direct metabolite identification.

Although elegant noninvasive magnetic resonance imaging techniques are illuminating metabolic processes in a range of organisms, including humans, these techniques are too complex and expensive to be of practical use in studies of microbial physiology (2, 3, 5, 7, 34). The usefulness of other NMR techniques with hydrogen (^{1}H), carbon (^{13}C), nitrogen (^{15}N), and phosphorus (^{31}P), the most studied and biologically important magnetic nuclei, may depend on certain conditions (7). ^{13}C and ^{15}N are of low natural abundance, making detection difficult unless specifically labeled compounds are used (8, 28). ^{31}P NMR is restricted to compounds that contain that nucleus, although interpretation of the spectra is simplified by the limited number of phosphorous-containing compounds. ^{1}H NMR has the opposite problem: the abundance of protonated compounds makes spectral interpretation impossible without filtering techniques. Single overwhelming signals, such as those in ^{1}H NMR resulting from H_2O, may be significantly reduced with presaturation pulses or magnetic field gradients, whereas multiple quantum coherence spectroscopy or spin echo approaches may be used to observe specific compounds in complex mixtures (12, 24, 34). In a few specialized cases it is possible to examine the appearance and disappearance of metabolites that are at high concentrations in the cells. However, the vast array of chemicals in cells and culture media are sufficiently alike in their ^{1}H NMR spectral characteristics to preclude metabolic studies of individual compounds without the addition of labels.

MO-NMR studies of natural-abundance ^{1}H compounds are easily accomplished with FT-NMR spectrometers using standard single-pulse sequences. In general, sufficient ^{1}H is present in the D_2O (1% ^{1}H is equivalent to approximately 1 M protons) to warrant using some means of water suppression, such as a presaturating pulse. Using a 300-MHz FT-NMR spectrometer and this approach, short data acquisition times of less than 5 min were sufficient to allow us to monitor the catabolism of natural ^{1}H, off-the-shelf compounds by fully deuterated *A. calcoaceticus* cultures and to detect metabolites at concentrations of approximately 50 μM. These approaches allow the direct observation of metabolite flow and may be successfully applied to studies of bacterial catabolism.

ACKNOWLEDGMENTS

This research was supported by National Science Foundation grant MCB-9507393 (to E.L.N.) and by NIH SBIR phase I grant 1R43 ESO 6304-01 (to G.L.G.). Additional support was provided (to E.L.N.) from the University of Georgia Research Foundation, Inc.

We gratefully acknowledge the Wheaton College Chemistry Department for interesting discussions and the use of their 300-MHz NMR spectrometer. We also thank L. N. Ornston for helpful discussions.

REFERENCES

1. **Ampe, F., and N. D. Lindley.** 1995. Acetate utilization is inhibited by benzoate in *Alcaligenes eutrophus*: evidence for transcriptional control of the expression of *acoE* coding for acetyl coenzyme A synthetase. J. Bacteriol. **177:**5826–5833.
2. **Avison, M. J., H. P. Hetherington, and R. G. Shulman.** 1986. Applications of NMR to studies of tissue metabolism. Annu. Rev. Biophys. Biophys. Chem. **15:**377–402.
3. **Bell, J. D., J. C. C. Brown, and P. J. Sadler.** 1989. NMR studies of body fluids. NMR Biomed. **2:**246–256.
4. **Bethesda Research Laboratories.** 1986. BRL pUC host: *E. coli* DH5α competent cells. Bethesda Res. Lab. Focus **8:**9–10.
5. **Campbell-Burk, S. L., and R. G. Shulman.** 1987. High-resolution NMR studies of *Saccharomyces cerevisiae*. Annu. Rev. Microbiol. **41:**595–616.
6. **Canovas, J. L., and R. Y. Stanier.** 1967. Regulation of the β-ketoadipate pathway in *Moraxella calcoaceticus*. Eur. J. Biochem. **1:**289–300.
7. **Cerdan, S., and J. Seelig.** 1990. NMR studies of metabolism. Annu. Rev. Biophys. Biophys. Chem. **19:**43–67.
8. **Cohen, S. M.** 1989. Enzyme regulation of metabolic flux. Methods Enzymol. **177:**417–434.
9. **Cohen-Bazire, G., W. R. Sistrom, and R. Y. Stanier.** 1957. Kinetic studies of pigment synthesis by non-sulfur purple bacteria. J. Cell. Comp. Physiol. **49:**25–68.
10. **Collier, L. S., and E. L. Neidle.** 1996. Characterization of BenM, a LysR-type transcriptional activator regulating benzoate degradation in *Acinetobacter calcoaceticus*, abstr. K-127. *In* Abstracts of the General Meeting of the American Society for Microbiology 1996. American Society for Microbiology, Washington, D.C.
11. **Crespi, H. L.** 1982. The isolation of deuterated bacteriohodopsin from fully deuterated *Halobacterium halobium*. Methods Enzymol. **88:**3–5.
12. **Dalvit, C., S. Y. Ko, and J. M. Bohlen.** 1996. Single and multiple-selective excitation combined with pulse-field gradients. J. Magn. Reson. **110:**124–131.
13. **DiMarco, A. A., B. Averhoff, and L. N. Ornston.** 1993. Identification of the transcriptional activator *pobR* and characterization of its role in the expression of *pobA*, the structural gene for *p*-hydroxybenzoate hydroxylase in *Acinetobacter calcoaceticus*. J. Bacteriol. **175:**4499–4506.
14. **Freibolin, H.** 1991. Basic one- and two-dimensional NMR spectroscopy. VCH Publishers, Weinheim, Germany.
15. **Gaines, G. L., III.** Unpublished data.
16. **Gralton, E. M.** 1996. Physical and genetic map of *Acinetobacter calcoaceticus* strain BD413(ADP1). M.S. thesis. University of Georgia, Athens.
17. **Harwood, C. S., and R. E. Parales.** 1996. The β-ketoadipate pathway and the biology of self-identity. Annu. Rev. Microbiol. **50:**553–590.
18. **Juni, E.** 1972. Interspecies transformation of *Acinetobacter*: genetic evidence for a ubiquitous genus. J. Bacteriol. **112:**917–931.
19. **Juni, E., and A. Janik.** 1969. Transformation of *Acinetobacter calco-aceticus* (*Bacterium anitratum*). J. Bacteriol. **98:**281–288.
20. **Katz, J. J., and H. L. Crespi.** 1966. Deuterated organisms: cultivation and uses. Science **151:**1187–1194.
21. **Neidle, E. L., C. Hartnett, and L. N. Ornston.** 1989. Characterization of *Acinetobacter calcoaceticus catM*, a repressor gene homologous in sequence to transcriptional activator genes. J. Bacteriol. **171:**5410–5421.
22. **Neidle, E. L., M. Shapiro, and L. N. Ornston.** 1987. Cloning and expression in *Escherichia coli* of *Acinetobacter calcoaceticus* genes for benzoate degradation. J. Bacteriol. **169:**5496–5503.
23. **Nichols, N. N., and C. S. Harwood.** 1995. Repression of 4-hydroxybenzoate transport and degradation by benzoate: a new layer of regulatory control in the *Pseudomonas putida* β-ketoadipate pathway. J. Bacteriol. **177:**7033–7040.
24. **Norwood, T. J.** 1994. Magnetic field gradients in NMR: friend or foe? Chem. Soc. Rev. **23:**59–66.

25. **Ornston, L. N., J. Houghton, E. L. Neidle, and L. A. Gregg.** 1990. Subtle selection and novel mutation during evolutionary divergence of the β-ketoadipate pathway, p. 207–225. *In* S. Silver, A. M. Chakrabarty, B. Iglewski, and S. Kaplan (ed.), *Pseudomonas*: biotransformations, pathogenesis, and evolving biotechnology. American Society for Microbiology, Washington, D.C.
26. **Ornston, L. N., and E. L. Neidle.** 1991. Evolution of genes for the β-ketoadipate pathway in *Acinetobacter calcoaceticus*, p. 201–237. *In* K. J. Towner, E. Bergogne-Berezin, and C. A. Fewson (ed.), The biology of *Acinetobacter*. Plenum Press, New York.
27. **Ornston, L. N., and R. Y. Stanier.** 1966. The conversion of catechol and protocatechuate to β-ketoadipate by *Pseudomonas putida*. I. Biochemistry. J. Biol. Chem. **241:**3776–3786.
28. **Pasternack, L. B., D. A. Laude, and D. R. Appling.** 1992. ^{13}C NMR detection of folate-mediated serine and glycine synthesis in vivo in *Saccharomyces cerevisiae*. Biochemistry **31:**8713–8719.
29. **Prentki, P., and H. M. Krisch.** 1984. In vitro insertional mutagenesis with a selectable DNA fragment. Gene **29:**303–313.
30. **Romero-Arroyo, C. E., M. A. Schell, G. L. Gaines III, and E. L. Neidle.** 1995. *catM* encodes a LysR-type transcriptional activator regulating catechol degradation in *Acinetobacter calcoaceticus*. J. Bacteriol. **177:**5891–5898.
31. **Sambrook, J., E. F. Fritsch, and T. Maniatis.** 1989. Molecular cloning: a laboratory manual, 2nd ed. Cold Spring Harbor Laboratory Press, Cold Spring Harbor, N.Y.
32. **Seeholzer, S. H., M. Cohn, J. A. Putkey, A. R. Means, and H. L. Crespi.** 1986. NMR studies of a complex of deuterated calmodulin with melittin. Proc. Natl. Acad. Sci. USA **83:**3634–3638.
33. **Shanley, M. S., E. L. Neidle, R. E. Parales, and L. N. Ornston.** 1986. Cloning and expression of *Acinetobacter calcoaceticus catBCDE* genes in *Pseudomonas putida* and *Escherichia coli*. J. Bacteriol. **165:**557–563.
34. **Skibsted, U., and P. E. Hansen.** 1990. ^{1}H NMR spin-echo spectroscopy of human erythrocytes. Transformation of exogenous compounds. NMR Biomed. **3:**248–258.
35. **Vieira, J., and J. Messing.** 1982. The pUC plasmids, an M13mp7-derived system for insertion mutagenesis and sequencing with synthetic universal primers. Gene **19:**259–268.
36. **Yanisch-Perron, C., J. Vieira, and J. Messing.** 1985. Improved M13 phage cloning vectors and host strains: nucleotide sequences of the M13mp18 and pUC19 vectors. Gene **33:**103–119.